

Stochastic Backgrounds of Gravitational Waves from Cosmological Sources: Techniques and Applications to Preheating

Larry R. Price* and Xavier Siemens†

*Center for Gravitation and Cosmology, Department of Physics,
University of Wisconsin–Milwaukee, P.O. Box 413, Milwaukee, Wisconsin 53201, USA*

Several mechanisms exist for generating a stochastic background of gravitational waves in the period following inflation. These mechanisms are generally classical in nature, with the gravitational waves being produced from inhomogeneities in the fields that populate the early universe and not quantum fluctuations. The resulting stochastic background could be accessible to next generation gravitational wave detectors. We develop a framework for computing such a background analytically and computationally. As an application of our framework, we consider the stochastic background of gravitational waves generated in a simple model of preheating.

I. INTRODUCTION

Prior to the time of recombination the universe is opaque to electromagnetic waves. The detection of a gravitational wave background generated before recombination would provide a unique observational window. Observations of this background would afford us rare and powerful probes of early universe physics and cosmology and could have profound implications.

The detection and study of gravitational waves is currently at the forefront of fundamental physics research. A world-wide network of gravitational wave detectors is poised to make the first detection. The Laser Interferometer Gravitational-Wave Observatory (LIGO) and the Virgo interferometer have already achieved unprecedented sensitivities at frequencies around 100 Hz and are currently undergoing upgrades. Future detectors such as Advanced LIGO and the Laser Interferometer Space Antenna (LISA) promise to provide even more sensitivity and allow for observations at other frequencies.

Inflation produces a stochastic background of gravitational waves through the amplification of primordial quantum fluctuations [1, 2]. Unfortunately this background is too weak to be directly detected with existing instruments. It might, however, be observed via B-modes in the cosmic microwave background (CMB) [3, 4]. In the period following inflation there are a number of mechanisms that could result in the production of an additional gravitational wave background; for example phase transitions [5, 6, 7, 8, 9, 10, 11], as well as reheating and preheating [12, 13, 14, 15, 16, 17, 18, 19, 20, 21, 22, 23, 24, 25, 26]. These mechanisms are generally classical in nature: The gravitational waves are generated through inhomogeneities in the various matter fields that populate the early universe. The gravitational waves produced by some of these mechanisms are close to being detectable by Advanced LIGO [17, 19], and well within the reach of LISA [27].

In many of these models the effects of the expansion of the universe cannot be neglected. The gravitational waves can be produced on time and length scales comparable to the Hubble scale. In this paper we develop a framework for computing gravitational wave backgrounds in such situations and apply it to a simple well-studied model of preheating.

The realization that preheating could lead to the efficient production of a gravitational wave background was first made by Khlebnikov and Tkachev [13]. They made an analytic estimate of the stochastic background produced by preheating in a quartic inflation model. To estimate the stochastic background they used a flat space formula due to Weinberg [28] for the energy in gravitational waves per unit solid angle. They found relatively large values of the background peaked at frequencies around $f \sim 10^8$ Hz. A similar estimate by Garcia-Bellido [17], showed that in hybrid inflation the frequency of the peak in the spectrum could be brought down to the 1 kHz range where Advanced LIGO might detect it. Almost a decade later, the problem was independently revisited by Garcia-Bellido and Figueroa [21] and Easter and Lim [19]. The former [21] studied hybrid inflation models using a flat space code that evolved the scalar fields as well as the metric perturbation. The latter [19] evolved the scalar fields in a Friedmann-Robertson-Walker universe using Felder and Tkachev's LATTICEASY [29], considered quartic as well as quadratic inflationary potentials, and used Weinberg's flat space formula. Easter, Giblin, and Lim [19, 23] later developed a new computational strategy to include the effects of cosmological expansion. They coupled LATTICEASY to an integrator for the equation for the metric perturbation (using a mode decomposition) which they used to study hybrid inflation models. They found that the amplitude of the background is energy scale independent, and confirmed the analytic estimates of Garcia-Bellido [17] showing hybrid inflation models might lead to a signal detectable by Advanced LIGO. Later, Garcia-Bellido, Figueroa, and Sastre [20] re-examined the problem in an expanding spacetime using LATTICEASY and a configuration space integrator for the metric perturbation. In the meantime Dufaux, Bergman, Felder, Kofman, and Uzan [22]

*Electronic address: larry@gravity.phys.uwm.edu

†Electronic address: siemens@gravity.phys.uwm.edu

studied the problem using Green's functions. They constructed an approximate Green's function valid for gravitational waves generated well inside the horizon for any kind of cosmological expansion. The methods we develop in this paper are most similar to this work.

In Section II, using a mode decomposition in the equation for the evolution of the metric perturbation, we construct *exact* Green's functions for radiation- and matter-dominated expansions. Since our Green's functions are exact we faithfully recover the perturbations at all wavelengths. We are, however, tied to particular types of expansion (radiation- or matter-dominated). We use these Green's functions to construct an analytic expression for the energy emitted in gravitational waves as a function the Fourier transform of the stress energy tensor (in conformal coordinates) analogous to Weinberg's flat space formula [28]. This expression is useful when the evolution of the fields is known as well as for analytic estimates. We also use these Green's functions to write down the energy density in gravitational waves in a form suitable for lattice simulations. In Section III we introduce the simple model of preheating that we use to validate our framework. This is followed by a prescription of how to translate the results of our simulations to values today. Finally we present and discuss our results. Our conclusions are found in Section IV.

II. THEORETICAL FRAMEWORK

In this section we will lay out the basic framework for computing stochastic backgrounds given some matter source ($T_{\mu\nu}$). We will start by solving the perturbed Einstein equations for radiation- and matter-dominated expansion using exact Green's functions in conformal coordinates. In Appendix A we provide these Green's functions in comoving coordinates. The metric perturbation determines the effective stress-energy tensor for gravitational waves, which, in turn, leads to an expression for the energy density in gravitational waves. We will develop this in both analytic and computational directions. On the analytic side we will provide a Weinberg-like formula for the energy in gravitational waves as a function of solid angle valid for expanding spacetimes. On the computational side, we will write down the same equations in a form useful for lattice simulations.

A. Metric perturbations: Conformal Coordinates

We will be primarily working in a spatially flat Friedmann-Robertson-Walker (FRW) metric in conformal coordinates:

$$ds^2 = a^2(\eta)(-d\eta^2 + dx^2 + dy^2 + dz^2). \quad (1)$$

Our interest is in the first order metric perturbation, $h_{\mu\nu}$. We choose to work in a spatial transverse-traceless

gauge [30] defined by

$$h_{\mu 0}^{\text{TT}} = 0, \quad (2)$$

$$\partial_i h_{ij}^{\text{TT}} = 0, \quad (3)$$

$$h_{ii}^{\text{TT}} = 0, \quad (4)$$

where μ is a spacetime index, $i, j = 1, 2, 3$ labels spatial indices and $\partial_i = \frac{\partial}{\partial x^i}$. The physical metric is then

$$ds^2 = a^2(\eta)[-d\eta^2 + (\delta_{ij} + h_{ij}^{\text{TT}})dx^i dx^j], \quad (5)$$

and the perturbed Einstein equations take on a particularly simple form:

$$\ddot{h}_{ij}^{\text{TT}} + 2\frac{\dot{a}(\eta)}{a(\eta)}\dot{h}_{ij}^{\text{TT}} - \nabla^2 h_{ij}^{\text{TT}} = 16\pi T_{ij}^{\text{TT}}, \quad (6)$$

where the overdot denotes the derivative with respect to conformal time, ∇^2 is the three dimensional Laplacian in Euclidean space and the TT superscript denotes the transverse-traceless projection described below.

For a generic perturbation of an arbitrary spacetime there is an inherent ambiguity in differentiating between the background and the perturbation. The ambiguity is essentially the gauge choice one makes when identifying points on the background spacetime with those on the physical (perturbed) spacetime [31]. For a spatially flat FRW background, where the expansion is driven by a perfect fluid source with comoving velocity u^μ , the full ("background + perturbation") stress-energy tensor is

$$T_{\mu\nu} = (\rho + p)u_\mu u_\nu + pg_{\mu\nu} + \pi_{\mu\nu}, \quad (7)$$

where ρ and p are the energy density and pressure, respectively, $g_{\mu\nu}$ is the metric of the background (FRW) spacetime and $\pi_{\mu\nu} = \pi_{\nu\mu}$ is the anisotropic stress¹. We consider the contribution of the anisotropic stress to be a perturbation of the otherwise homogeneous and isotropic background (with the expansion sourced by the first two terms in Eq. (7)). The anisotropic stress tensor satisfies $u^\mu \pi_{\mu\nu} = \pi^\mu{}_\mu = 0$, so it is both purely spatial and traceless. In this situation it is clear that the only surviving term under the (spatial) transverse-traceless projection is π_{ij}^{TT} , so this choice of gauge provides an unambiguous splitting of the (homogeneous) background and the perturbation. For this paper we will be working exclusively in the TT gauge and will thus simply write our source term as T_{ij}^{TT} .

Solving Eq. (6) is easiest if we first perform a spatial Fourier transform while leaving the dependence on conformal time unchanged. Our convention for the Fourier transform is given by

$$f(\eta, \mathbf{x}) = \frac{1}{(2\pi)^2} \int_{-\infty}^{\infty} d\omega d^3\mathbf{k} e^{-i(\omega\eta - \mathbf{k}\cdot\mathbf{x})} f(\omega, \mathbf{k}). \quad (8)$$

¹ Some authors write $\pi_{\mu\nu} = a^2\Pi_{\mu\nu}$ in FRW backgrounds.

The perturbed Einstein equations then become

$$\ddot{h}_{ij}^{\text{TT}}(\eta, \mathbf{k}) + 2\frac{\dot{a}(\eta)}{a(\eta)}\dot{h}_{ij}^{\text{TT}}(\eta, \mathbf{k}) + \omega^2 h_{ij}^{\text{TT}}(\eta, \mathbf{k}) = 16\pi T_{ij}^{\text{TT}}(\eta, \mathbf{k}), \quad (9)$$

with $\omega^2 = \mathbf{k} \cdot \mathbf{k}$.

The transverse-traceless projection is easily described in momentum space. The TT part of some spatial tensor, T_{ij} , is given by [30]

$$T_{ij}^{\text{TT}}(\mathbf{k}) = \{P_{im}(\mathbf{k})P_{jn}(\mathbf{k}) - \frac{1}{2}P_{ij}(\mathbf{k})P_{mn}(\mathbf{k})\}T_{mn}(\mathbf{k}), \quad (10)$$

where

$$P_{ij}(\mathbf{k}) = \delta_{ij} - \frac{k_i k_j}{\omega^2}. \quad (11)$$

In order to solve for the metric perturbation, we must know something about the evolution of the scale factor. We will consider the two cases

$$a(\eta) = \alpha\eta \quad \text{and} \quad a(\eta) = \alpha\eta^2, \quad (12)$$

which correspond to radiation- and matter-dominated expansion, respectively, for some constant α . The solution in terms of a Green's function is given quite simply by

$$h_{ij}^{\text{TT}}(\eta, \mathbf{k}) = \frac{16\pi}{\omega\eta} \int_{\eta_i}^{\eta} d\eta' \eta' \sin[\omega(\eta - \eta')] T_{ij}^{\text{TT}}(\eta', \mathbf{k}), \quad (13)$$

for radiation-dominated expansion and

$$h_{ij}^{\text{TT}}(\eta, \mathbf{k}) = \frac{16\pi}{(\omega\eta)^3} \int_{\eta_i}^{\eta} d\eta' \eta' \left\{ (1 + \omega^2 \eta \eta') \sin[\omega(\eta - \eta')] - \omega(\eta - \eta') \cos[\omega(\eta - \eta')] \right\} \times T_{ij}^{\text{TT}}(\eta', \mathbf{k}), \quad (14)$$

for matter-dominated expansion. The lower limit of integration in both Eqs. (13) and (14) is determined by the time the source turns on, η_i . The upper limit is $\eta_{<} \equiv \min(\eta, \eta_f)$, where η is the time the source is being computed and η_f is the time the source turns off.

It is interesting to note that both types of expansion lead to relatively simple (and similar) expressions. This is a result of the fact that we are working in momentum space. In configuration space the Green's function for radiation-dominated expansion only has support on the light-cone. The matter-dominated expansion Green's function contains a "tail" term that has support *inside* the past lightcone [32]. This severely complicates a configuration space computation of the metric perturbation.

B. Energy density in gravitational radiation

The effective stress-energy tensor for gravitational radiation is given covariantly (in a transverse-traceless

gauge) by [30]

$$T_{\mu\nu}^{\text{gw}} = \frac{1}{32\pi} \left\langle \nabla_\mu \gamma_{\alpha\beta}^{\text{TT}} \nabla_\nu \gamma^{\alpha\beta \text{TT}} \right\rangle, \quad (15)$$

where $\gamma_{\mu\nu}$ is the metric perturbation ($g_{\mu\nu} = g_{\mu\nu}^{\text{background}} + \gamma_{\mu\nu}$) and the angle brackets denote a spatial average over several wavelengths and the covariant derivative is compatible with the background metric. When working with this expression we must be careful to remember that according to Eq. (5) $\gamma_{\mu\nu}^{\text{TT}} = a^2 h_{ij}^{\text{TT}}$.

The quantity of interest for stochastic background computations is the energy density in gravitational waves, ρ_{gw} . Though it is rarely stated explicitly, ρ_{gw} is defined with respect to the proper time of a co-moving observer at rest, i.e.,

$$\rho_{\text{gw}} \equiv t^\mu t^\nu T_{\mu\nu}^{\text{gw}}(t, \mathbf{x}), \quad (16)$$

where $t^\mu = (1, 0, 0, 0)$ in the (background) metric

$$ds^2 = -dt^2 + a^2(t) d\vec{x} \cdot d\vec{x}. \quad (17)$$

Transforming to conformal coordinates:

$$\begin{aligned} \rho_{\text{gw}} &= t^\mu t^\nu T_{\mu\nu}^{\text{gw}}(t, \mathbf{x}) \\ &= \frac{\eta^\mu \eta^\nu}{a^2(\eta)} T_{\mu\nu}^{\text{gw}}(\eta, \mathbf{x}) \\ &= \frac{\eta^\mu \eta^\nu}{32\pi a^2(\eta)} \sum_{i,j} \left\langle \nabla_\mu [a^2(\eta) h_{ij}^{\text{TT}}] \nabla_\nu [h_{ij}^{\text{TT}} / a^2(\eta)] \right\rangle \\ &= \frac{1}{32\pi a^2(\eta)} \sum_{i,j} \left\langle \dot{h}_{ij}^{\text{TT}}(\eta, \mathbf{x}) \dot{h}_{ij}^{\text{TT}}(\eta, \mathbf{x}) \right\rangle, \end{aligned} \quad (18)$$

where $\eta^\mu = (1, 0, 0, 0)$ in conformal coordinates. Performing the spatial averaging and using Parseval's theorem we obtain

$$\rho_{\text{gw}} = \frac{1}{32\pi a(\eta)^2} \frac{1}{V} \sum_{i,j} \int d^3\mathbf{k} \left| \dot{h}_{ij}^{\text{TT}}(\eta, \mathbf{k}) \right|^2 \quad (19)$$

where V is the comoving volume over which the average is being performed. We will use this result in both analytic and computational contexts, which we develop separately in the next two subsections.

It is important to note that not all modes of the perturbations we have been discussing are gravitational waves in the technical sense. Gravitational waves only exist as such when the typical wavelength of metric perturbations is much smaller than the characteristic length scale of the background spacetime, which in the present context is the Hubble radius. In other words, waves can only be observed in situations where a wave zone is well-defined. In the current situation, this only happens after the universe has expanded significantly, e.g., today. Thus, in order to correctly apply the formalism developed in the remainder of this section, a (generally model dependent) procedure must be prescribed for "transferring" the value of ρ_{gw} at the time of creation to today's values (see Section III B for an example).

C. Weinberg-like formula

Perhaps the most often used tool for analytic calculations of gravitational radiation is the the formula that appears in Weinberg [28] for the energy in gravitational radiation, E_{gw} , as a function of solid angle²

$$\frac{dE_{\text{gw}}}{d\Omega} = \pi^2 \sum_{i,j} \int_{-\infty}^{\infty} d\omega \omega^2 |T_{ij}^{\text{TT}}(\omega, \mathbf{k})|^2. \quad (20)$$

Though the formula is simple its usefulness is limited to applications in Minkowski space. It is straightforward to derive similar expressions for use in radiation- and matter-dominated (spatially flat) FRW spacetimes.

Imagine that our source, T_{ij}^{TT} , is only active for some finite period of time before “turning off”. Then we are free to take the upper and lower limits of Eq. (13) to infinity. At the same time, we can write the source as $T_{ij}^{\text{TT}}(\omega, \mathbf{k})$ using the inverse Fourier transform defined in Eq. (8). Interchanging the η and ω integrals then leads to

$$h_{ij}^{\text{TT}}(\eta, \mathbf{k}) = -i\sqrt{512\pi^3} \frac{\sin(\omega\eta)}{\omega\eta} \frac{\partial}{\partial\omega} T_{ij}^{\text{TT}}(\omega, \mathbf{k}) \quad (21)$$

It follows directly that

$$\dot{h}_{ij}^{\text{TT}}(\eta, \mathbf{k}) = i\sqrt{512\pi^3} \frac{\sin(\omega\eta) - \omega\eta \cos(\omega\eta)}{\omega\eta^2} \frac{\partial}{\partial\omega} T_{ij}^{\text{TT}}(\omega, \mathbf{k}) \quad (22)$$

Using these expressions and setting $a(\eta) = \alpha\eta$ in Eq. (19), we have

$$\begin{aligned} \frac{dE_{\text{gw}}}{d\Omega} &= \frac{16\pi^2}{\alpha^2\eta^6} \int_{-\infty}^{\infty} d\omega [\sin(\omega\eta) - \omega\eta \cos(\omega\eta)]^2 \\ &\quad \times \left| \frac{\partial}{\partial\omega} T_{ij}^{\text{TT}}(\omega, \mathbf{k}) \right|^2. \end{aligned} \quad (23)$$

A similar expression holds for the case of matter-dominated expansion.

D. Computational methods

In many situations, such as the one we will consider in the next section, the source of gravitational radiation contains a nonlinear interaction term and we must resort to computer simulations for a result. The quantity of interest is given in conformal coordinates by

$$\frac{d\rho_{\text{gw}}}{d\ln\omega} = \frac{\omega^3}{32\pi a^2(\eta)} \frac{1}{V} \sum_{i,j} \int d\Omega \left| \dot{h}_{ij}^{\text{TT}}(\eta, \mathbf{k}) \right|^2. \quad (24)$$

² We have an extra factor of π^2 relative to the formula in Weinberg’s book [28] due to our Fourier transform convention [see our Eq. (8)].

This expression follows directly from Eq. (19) and is proportional to Ω_{gw} , the ratio of energy density in gravitational waves to the energy density required to close the universe. In practice, the integral over solid angle requires one to sum over the entire cubic lattice, which is an $\mathcal{O}(N^3)$ operation, where N is the number of lattice points in each direction.

In some situations, to reduce the computational complexity, a trick introduced in [22] may be used. If we assume the stochastic background is isotropic, we can perform the integral analytically along any particular direction. That is, we can write

$$\frac{d\rho_{\text{gw}}}{d\ln\omega} = \frac{\omega^3}{8a^2(\eta)} \frac{1}{V} \sum_{i,j} \left| \dot{h}_{ij}^{\text{TT}}(\eta, \omega \hat{\mathbf{k}}_{\mathbf{p}}) \right|^2, \quad (25)$$

where $\hat{\mathbf{k}}_{\mathbf{p}}$ is a unit vector in the direction we have chosen. In practice there are direction dependent statistical fluctuations but these can be reduced by averaging Eq. (25) over several directions. There is a slight subtlety involved: For a cubic lattice with N^3 points, the maximum length (in momentum space) of any component of \mathbf{k} is proportional to $N/2$, so that in three dimensions the maximum possible length of \mathbf{k} is $\omega_{\text{max}} \propto \sqrt{3}(N/2)$. However, the length along any particular direction is generally shorter than this so the task is to try and maximize both ω_{max} and the number of directions with that maximum length ω_{max} . Following [22], we choose six face diagonals of the cube. Namely, the directions that run diagonally across the x - y , x - z , y - z , $(-x)$ - y , $(-x)$ - z and $(-y)$ - z planes. This leads to a reasonable reduction in the effect of statistical fluctuations, with $\omega_{\text{max}} \propto \sqrt{2}(N/2)$. Further details of our computational methods are given in Appendix B.

III. EXAMPLE: PREHEATING

In this section we will consider, as an application of our formalism, the stochastic background generated from a simple model of preheating after inflation. This is an active subject that has been studied with various techniques, which makes it ideal for validating our methods. We will start with a brief introduction to the physics of preheating. Then we will discuss how one uses the output of the simulation to determine the spectrum of the stochastic background today before providing a discussion of our results.

A. Background

At the end of inflation the universe is very cold and far from thermal equilibrium, which poses a challenge for the hot big bang scenario.

The earliest attempts at describing reheating after inflation were centered on the idea that the oscillations of the inflaton about its minimum produce standard model

particles that then interact and bring the universe into thermal equilibrium [33, 34, 35, 36]. It was later discovered that this process is preceded by a stage of exponential particle production which became known as preheating [12, 15, 37].

We will consider a simple model of preheating in which the inflaton, ϕ , is coupled to some scalar field, χ , according to the Lagrangian

$$\mathcal{L} = \sqrt{-g} \left(\frac{1}{2} \nabla_\mu \phi \nabla^\mu \phi + \frac{1}{2} \nabla_\mu \chi \nabla^\mu \chi - V(\phi, \chi) \right), \quad (26)$$

where $V(\phi, \chi)$ contains both the inflationary potential and the coupling between the two fields. In this work we will limit our consideration to

$$V(\phi, \chi) = \frac{g^2}{2} \phi^2 \chi^2 + \frac{\lambda}{4} \phi^4. \quad (27)$$

The coupling term between ϕ and χ in Eq. (26) enters the Lagrangian as a spacetime dependent mass term for both fields. This non-linear term can produce an effect known as parametric resonance. Perhaps the most familiar example of parametric resonance is that of a child on a swing at the playground. The child, essentially a pendulum, learns fairly quickly if she swings her legs back and forth, effectively changing the length of the pendulum in a time-dependent manner, that she can swing higher and higher, having driven the system into resonance.

A more precise description of the dynamics is given by [14], which is partially summarized in the following. At the end of inflation, the χ field starts off with zero amplitude and the oscillations of the inflaton about its minimum are described in terms of a conformally rescaled field $\varphi = a\phi$ by the equation

$$\ddot{\varphi} + \lambda \varphi^3 = 0, \quad (28)$$

which has as its solution the Jacobi elliptic cosine function

$$\varphi = \frac{x}{\eta\sqrt{\lambda}} \operatorname{cn} \left(x - x_0, \frac{1}{\sqrt{2}} \right), \quad (29)$$

where $x = \eta\phi_0\sqrt{\lambda}$ and ϕ_0 is the initial value of the inflaton. The evolution of the k -modes of the conformally rescaled $X_k = a\chi_k$ is described by (the Lamé equation)

$$\ddot{X}_k + \left[\frac{k^2}{\lambda\phi_0^2} + \frac{g^2}{\lambda} \operatorname{cn} \left(x - x_0, \frac{1}{\sqrt{2}} \right) \right] X_k = 0. \quad (30)$$

This is essentially the harmonic oscillator with a time-dependent frequency given by the term in square brackets. The combination $g^2/\lambda \equiv q$ governs the strength of the time-dependent term in the frequency and is generally called the resonance parameter. In our simulations we typically use $q \sim 100$, which results in complicated dynamics. The coupling between χ and the inflaton means

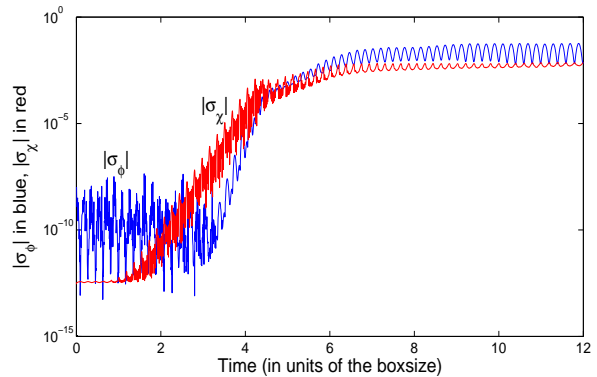


FIG. 1: Variances of ϕ and χ fields, as computed by LATTICEEASY. Note that these units do not account for the expansion of the universe.

that once the oscillations of the inflaton excite parametric resonance in χ , it in turn brings the inflaton into a stage of parametric resonance, which continues until this process becomes inefficient. This is seen quite clearly in Fig. 1, which shows the variances of each of the fields as a function of time for one of our simulations (described in Section III C). Though the variances themselves are of no particular interest, they provide a simple way to visualize the time evolution of the full three dimensional dynamics.

B. Values today

As discussed in Section II B, we need a prescription for translating metric perturbations in the early universe into gravitational radiation today. Our discussion of the transfer function, included for completeness, follows [22, 23]. Gravitational energy density scales like a^{-4} so that

$$a_0^4 \rho_{\text{gw},0} = a_e^4 \rho_{\text{gw},e}, \quad (31)$$

where the 0 and e subscripts denote today and the end of our simulations, respectively. Similarly, if entropy is conserved then radiation energy density scales like [38]

$$a_0^4 g_0^{1/3} \rho_{\text{rad},0} = a_e^4 g_e^{1/3} \rho_{\text{rad},e}, \quad (32)$$

where g_0 and g_e are the number of relativistic species today and at the end time of our simulation (we take $g_e/g_0 = 100$ for GUT scale inflation) and the energy density in radiation at the end of our simulations is, in the case of radiation-dominated expansion, just the total energy density at the end of the simulation (i.e., $\rho_{\text{rad},e} = \rho_{\text{tot},e}$). The quantity of interest is actually

$$\Omega_{\text{gw}} h^2 = \frac{1}{\rho_{\text{crit}}} \frac{d\rho_{\text{gw}}}{d \ln \omega}, \quad (33)$$

where $\rho_{\text{crit}} = 3H_0^2/8\pi$ is the critical density required to close the universe and h is a dimensionless factor that

accounts for the uncertainty in the value of the Hubble expansion rate today so that $\Omega_{\text{gw}}h^2$ is independent of this uncertainty. We can then use Eqs. (31) and (32) to write

$$\begin{aligned}\Omega_{\text{gw},0}h^2 &= \Omega_{\text{rad},0}h^2 \left(\frac{g_0}{g_e}\right)^{1/3} \frac{1}{\rho_{\text{tot},e}} \frac{d\rho_{\text{gw},e}}{d\ln\omega} \\ &\approx \frac{9.3 \times 10^{-6}}{\rho_{\text{tot},e}} \frac{d\rho_{\text{gw},e}}{d\ln\omega},\end{aligned}\quad (34)$$

after inserting the appropriate values. Similarly, we want the physical frequency today, $f_0 = \omega_0/2\pi = \omega_e/2\pi a_0$, which is easily obtained using Eq. (32)

$$\begin{aligned}f_0 &= \frac{\omega_e}{2\pi a_0} \\ &= \frac{\omega_e}{2\pi a_e} \left(\frac{g_0}{g_e}\right)^{1/12} \left(\frac{\rho_{\text{rad},0}}{\rho_{\text{rad},e}}\right)^{1/4} \\ &\approx \frac{\omega_e}{a_e \rho_{\text{tot},e}^{1/4}} (4 \times 10^{10} \text{ Hz}).\end{aligned}\quad (35)$$

The same expressions are found in [22] and [23].

C. Results

As stated previously, we use LATTICEEASY for the evolution of the scalar fields. Conveniently, the two field model specified by Eq. (26) is already setup in LATTICEEASY. For our comparison we used the same parameters as many of the simulations published in [22] and [23]. We took $\lambda = 10^{-14}$ and $g^2 = 1.2 \times 10^{-12}$, which sets the resonance parameter $q = 120$. The initial values of the fields are $\phi_0 = 0.342M_p$ and $\chi_0 = 0$, where M_p is the Planck mass. This choice of parameters sets $\lambda\phi_0^4/4 \sim (10^{15}\text{GeV})^4$, which means inflation happens at the GUT scale. Additionally, LATTICEEASY sets initial fluctuations of the fields as described in [29]. In conformal Planck units we took our box size to be $L = 20$, evolved the box for a time $\eta_f = 240$ using timesteps $\Delta\eta = 0.01$, and took $N = 256$ points along each of the three axis (the typical size used in previous publications). We are able to run this simulation, including gravitational wave computations, in 18 hours on a four core 3 GHz machine. The details of our implementation can be found in Appendix B.

Figure 2 shows the self-consistent evolution of the scale factor as a function of time (the preferred unit for time in all of our plots is the box size of the simulation). The straight line indicates that the expansion is radiation-dominated throughout the course of the simulation. More importantly, it validates our use of the radiation era Green's function.

To compute the stochastic background spectrum we use Eq. (34). The value of $\rho_{\text{tot},e}$ is computed by LATTICEEASY. To estimate $d\rho_{\text{gw},e}/d\ln\omega$ we use Eq. (25) computed along six different directions as described at

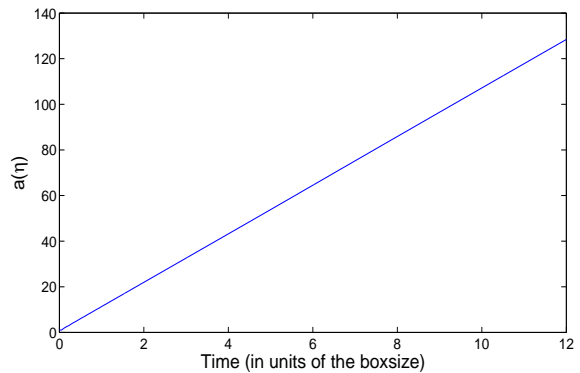


FIG. 2: Evolution of the scale factor as a function of time, computed by LATTICEEASY. Note that, to an extremely good approximation, the evolution is completely radiation-dominated.

the end of Section IID. Since the evolution is very well described by radiation-dominated expansion the values of $\hat{h}_{ij}^{\text{TT}}(\eta, \omega \hat{\mathbf{k}}_{\mathbf{p}})$ are updated at each time-step using

$$\begin{aligned}\hat{h}_{ij}^{\text{TT}}(\eta, \omega \hat{\mathbf{k}}_{\mathbf{p}}) &= \frac{16\pi}{\omega\eta} \int_{\eta_i}^{\eta} d\eta' \eta' \left\{ \omega \cos[\omega(\eta - \eta')] \right. \\ &\quad \left. - \frac{1}{\eta} \sin[\omega(\eta - \eta')] \right\} \\ &\quad \times T_{ij}^{\text{TT}}(\eta', \omega \hat{\mathbf{k}}_{\mathbf{p}})\end{aligned}\quad (36)$$

which follows from Eq. (13). We do this integral using the rectangle method which appears to be sufficient. To compute $T_{ij}^{\text{TT}}(\eta', \omega \hat{\mathbf{k}}_{\mathbf{p}})$ at each time-step we construct the six independent components of the spatial part of the stress energy tensor and Fourier transform them. Then we project out everything but the transverse-traceless part using Eqs. (10) and (11) for each of the six $\hat{\mathbf{k}}_{\mathbf{p}}$ we have previously chosen. The frequencies are given by Eq. (35) with $\omega_e = 2\pi i\sqrt{2}/L$, where $i = 1 \dots N/2$ (the factor of $\sqrt{2}$ comes from our choice of $\hat{\mathbf{k}}_{\mathbf{p}}$ along the face diagonals of the simulation box; see Section IID for details).

Fig. 3 shows the result of this procedure. We plot $\Omega_{\text{gw}}h^2$ as a function of frequency (both are the values today). The thin colored lines are the results along each of the six directions in momentum space and the thick black line is the average.

Next we present a comparison of our results with those obtained by other groups using different methods. The authors of [22], [23], and [20] kindly provided us with the results of their simulations. The (solid) black curve is the result of our simulation (the same as in Fig. 3). The (dash-dotted) blue curve is produced from the data published in [22]³. The (dashed) green curve shows the

³ These authors provided us with Ω_{gw} along each axis in addition

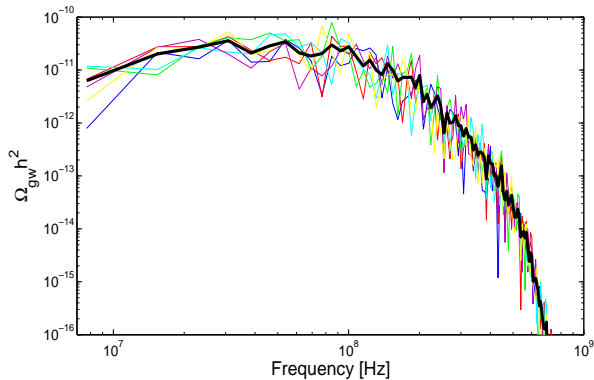


FIG. 3: The spectrum of the stochastic background today, $\Omega_{\text{gw}} h^2$, computed along six directions on the lattice (thin colored lines), and the average (thick black line).

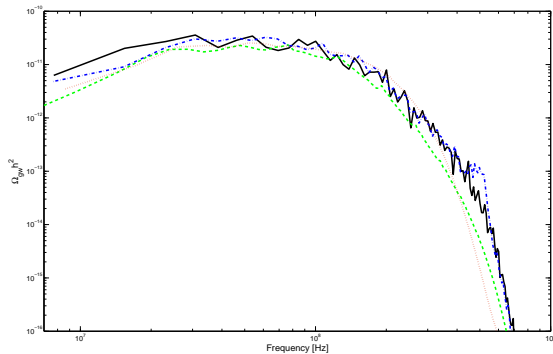


FIG. 4: Comparison of Ω_{gw} today as computed by the method described in this paper (solid black line), as well as the curves published in [22] (dash-dotted blue line), [23] (dashed green line) and [20] (dotted red line). Note the good agreement across methods.

simulation results published in [23] for higher resolution simulation with $N = 512$ points in each direction. Finally, the (dotted) red curve is from [20] for a simulation with $N = 128^4$. The results across all methods are in very good agreement.

It is worth pointing out that the Green’s function introduced in [22] is an approximation for general kinds of expansion, but for radiation-dominated expansion it is in fact exact. Looking at Eq. (12) of [22] we see that it is the same as our Eq. (13) (their metric perturbation is re-scaled by a factor of $a(\eta)$). However, they work in the small wavelength approximation and perform an additional average over a single period of oscillation, which

presumably accounts for the slight differences between the (dash-dotted) blue and (solid) black curves.

Although the results methods agree quite well with one another, there is a general issue common to all simulations: The fact that $\eta_f = 12L$. This, by itself, is not a problem, but LATTICEEASY uses periodic boundary conditions. This means that excitations of the scalar fields leave and re-enter the simulation box multiple times, setting up correlations in the field values not present in the early universe. The magnitude and importance of this effect is unclear. The problem can be avoided by setting the final time to (at most) half of the light-crossing time of the box, i.e., $\eta_f \leq L/2$. Keeping the same final time, $\eta_f = 240$, we would set $L = 480$, which would require 24^3 times as many points on the lattice to keep the current resolution. This, in turn would increase the memory required for the simulation by a similar factor. Alternatively, a glance at Fig. 1 suggests that gravitational wave production is essentially complete by $\eta = 120$ (this can be verified directly by monitoring the evolution in time of Ω_{gw}). A simulation with $\eta_f = 120$ and $L = 240$ would only require 12^3 times as many points to maintain the current resolution. We leave this investigation for future work.

Finally, an obvious question that arises is what to do in situations where there is significant gravitational wave production during times when the expansion of the universe is not purely radiation- or matter-dominated. While each situation requires its own analysis, we can, generally speaking, combine our method with that of [22]. That is, we can divide the calculation of Ω_{gw} into periods when the evolution is radiation- or matter-dominated and use the exact Green’s functions during those periods. In the periods in-between, where the evolution is more complicated, we can use the approximate expressions in [22].

IV. CONCLUSIONS

In this paper we have presented a method for computing the stochastic background of gravitational waves due to (classical) sources in a spatially flat FRW background. Our method centers around “evolving” the metric perturbation using the exact Green’s functions for radiation- and matter-dominated expansion. We developed these results into a Weinberg-like formula, applicable in expanding spacetimes, for use in situations where the dynamics of the source is known or can be approximated. Additionally, we used the same results to present a computational framework applicable to scalar field sources with complicated dynamics. Because our framework relies on Green’s functions for the evolution of the metric perturbation, it is robust and simple and we avoid the numerical difficulties associated with more complicated evolution schemes. Furthermore, we have shown that the results of using this framework to compute the stochastic background produced in the $\lambda\phi^4$ model of preheating agree quite well with those appearing in the literature.

to the six directions described in Section II D. Only the latter was used in Fig. 4

⁴ These authors provided us with $\Omega_{\text{gw}}/\rho_{\text{tot},e}$ and k at the end of the simulation. Fig. 4 displays the result of applying the transfer functions described in Section III B to their data.

While the frequency ranges and sensitivities of the gravitational waves from the model of preheating studied here make it unlikely to be detected in the near future, there remain several other options for the production of gravitational waves that could be observable soon. Aside from the sources discussed in Section I that may be observable to Advanced LIGO, phase transitions taking place at the electroweak scale could lead to a signal detectable by LISA [39]. We plan to investigate this in more detail using the methods introduced here.

Acknowledgments

We would like to thank John T. “Tom” Giblin, Jr. and Jolien Creighton for illuminating discussions. We would also like to thank Juan Garcia-Bellido, Jeff Dufaux, Richard Easther, Gary Felder, Dani Figueroa, Lev Kofman and Alfonso Sastre for useful communications. We are further grateful to Gary Felder and Igor Tkachev for developing LATTICEEASY and making it publicly available. LP is supported by NSF PHY-0503366 and the Research Growth Initiative at the University of Wisconsin-Milwaukee.

APPENDIX A: METRIC PERTURBATIONS IN COSMOLOGICAL TIME

In this appendix we derive expressions for the metric perturbation in the commonly used coordinates

$$ds^2 = -dt^2 + a^2(t)(\delta_{ij} + h_{ij}^{\text{TT}})dx^i dx^j, \quad (\text{A1})$$

for matter-dominated expansion.

APPENDIX B: COMPUTATIONAL DETAILS

Our code for computing the stochastic background interfaces directly with LATTICEEASY. We ran our simulations on a four core 3 GHz machine. To take advantage of the multi-processing capabilities available to us we used OpenMP [40] as implemented in gcc version 4.2.3. The loops over the lattice necessary to evaluate the six independent components of T_{ij} were split into four threads, each evaluated on one core. The most computationally

where $h_{ij}^{\text{TT}} = h_{ij}^{\text{TT}}(t, \mathbf{x})$ satisfies Eqs. (2–4). One could, in principle, perform a coordinate transformation on the expressions in conformal coordinates, but we find it more convenient to simply re-derive the results. In these coordinates the perturbed Einstein equations take the form (after performing a spatial Fourier transform):

$$h_{ij}^{\prime\prime \text{TT}} + 3\frac{a'(t)}{a(t)}h_{ij}^{\prime \text{TT}} + \frac{\omega^2}{a^2(t)}h_{ij}^{\text{TT}} = 16\pi\frac{T_{ij}^{\text{TT}}}{a^2(t)}. \quad (\text{A2})$$

Radiation- and matter-dominated expansion are characterized by

$$a(t) = \alpha t^{1/2} \quad \text{and} \quad a(t) = \alpha t^{2/3},$$

respectively, for some α . The Green’s functions give

$$h_{ij}^{\text{TT}}(t, \mathbf{k}) = \frac{16\pi}{\alpha^2\omega t^{1/2}} \int_{t_i}^{t_f} dt' \sin[2\omega(t^{1/2} - t'^{1/2})] T_{ij}^{\text{TT}}(t', \mathbf{k}), \quad (\text{A3})$$

for radiation-dominated expansion and

$$h_{ij}^{\text{TT}}(t, \mathbf{k}) = \frac{16\pi}{9\alpha^2\omega^3 t} \int_{t_i}^{t_f} dt' t'^{-1/3} \left\{ [1 + 9\omega^2 (tt')^{1/3}] \sin[3\omega(t^{1/3} - t'^{1/3})] - 3\omega(t^{1/3} - t'^{1/3}) \cos[3\omega(t^{1/3} - t'^{1/3})] \right\} T_{ij}^{\text{TT}}(t', \mathbf{k}), \quad (\text{A4})$$

expensive tasks we perform are the Fourier transforms of T_{ij} [see Eqs. (13) and (14)]. There are six Fourier transforms to perform at each timestep. For this task we enlist the help of the Fastest Fourier Transform in the West (FFTW) [41]. Although FFTW has its own multi-processor capabilities, we find that we can get $\sim 10\%$ better performance using OpenMP for the task. By trial and error we found six threads, one for each Fourier transform, to be the fastest option. Note that we have not modified LATTICEEASY. With these improvements the gravitational wave computation takes roughly the same amount of time as the field evolution. The simulation described in Section III C takes 18 hours to complete.

-
- [1] A. A. Starobinsky, JETP Lett. **30**, 682 (1979).
- [2] B. Allen, Phys. Rev. **D37**, 2078 (1988).
- [3] D. N. Spergel et al. (WMAP), Astrophys. J. Suppl. **170**, 377 (2007), astro-ph/0603449.
- [4] H. Peiris and R. Easther, JCAP **0610**, 017 (2006), astro-ph/0609003.
- [5] A. Kosowsky, M. S. Turner, and R. Watkins, Phys. Rev. **D45**, 4514 (1992).
- [6] A. Kosowsky, M. S. Turner, and R. Watkins, Phys. Rev. Lett. **69**, 2026 (1992).
- [7] A. Kosowsky and M. S. Turner, Phys. Rev. **D47**, 4372 (1993), astro-ph/9211004.
- [8] L. M. Krauss, Phys. Lett. **B284**, 229 (1992).
- [9] M. Kamionkowski, A. Kosowsky, and M. S. Turner, Phys. Rev. **D49**, 2837 (1994), astro-ph/9310044.
- [10] A. Kosowsky, A. Mack, and T. Kahniashvili, Phys. Rev. **D66**, 024030 (2002), astro-ph/0111483.
- [11] G. Felder, J. Garcia-Bellido, P. B. Greene, L. Kofman, A. Linde, and I. Tkachev, Phys. Rev. Lett. **87**, 011601 (2001).
- [12] L. Kofman, A. D. Linde, and A. A. Starobinsky, Phys. Rev. Lett. **73**, 3195 (1994), hep-th/9405187.
- [13] S. Y. Khlebnikov and I. I. Tkachev, Phys. Rev. **D56**, 653 (1997), hep-ph/9701423.
- [14] P. B. Greene, L. Kofman, A. D. Linde, and A. A. Starobinsky, Phys. Rev. **D56**, 6175 (1997), hep-ph/9705347.
- [15] L. Kofman, A. D. Linde, and A. A. Starobinsky, Phys. Rev. **D56**, 3258 (1997), hep-ph/9704452.
- [16] J. Garcia-Bellido and A. D. Linde, Phys. Rev. **D57**, 6075 (1998), hep-ph/9711360.
- [17] J. Garcia-Bellido (1998), hep-ph/9804205.
- [18] R. Easther and E. A. Lim, JCAP **0604**, 010 (2006), astro-ph/0601617.
- [19] R. Easther, J. Giblin, John T., and E. A. Lim, Phys. Rev. Lett. **99**, 221301 (2007), astro-ph/0612294.
- [20] J. Garcia-Bellido, D. G. Figueroa, and A. Sastre, Phys. Rev. **D77**, 043517 (2008), 0707.0839.
- [21] J. Garcia-Bellido and D. G. Figueroa, Phys. Rev. Lett. **98**, 061302 (2007), astro-ph/0701014.
- [22] J. F. Dufaux, A. Bergman, G. N. Felder, L. Kofman, and J.-P. Uzan, Phys. Rev. **D76**, 123517 (2007), 0707.0875.
- [23] R. Easther, J. Giblin, John T., and E. A. Lim (2007), 0712.2991.
- [24] R. Easther, J. T. Giblin, E. A. Lim, W.-I. Park, and E. D. Stewart (2008), 0801.4197.
- [25] C. Caprini, R. Durrer, and G. Servant (2007), 0711.2593.
- [26] K. Jones-Smith, L. M. Krauss, and H. Mathur, Phys. Rev. Lett. **100**, 131302 (2008), 0712.0778.
- [27] C. J. Hogan, AIP Conf. Proc. **873**, 30 (2006), astro-ph/0608567.
- [28] S. Weinberg, *Gravitation and Cosmology: Principles and Applications of the General Theory of Relativity* (Wiley, New York, U.S.A., 1972).
- [29] G. N. Felder and I. Tkachev (2000), hep-ph/0011159.
- [30] C. W. Misner, K. S. Thorne, and J. A. Wheeler, *Gravitation* (Freeman, 1973), san Francisco 1973, 1279p.
- [31] J. M. Stewart and M. Walker, Proc. Roy. Soc. Lond. **A341**, 49 (1974).
- [32] R. R. Caldwell, Phys. Rev. **D48**, 4688 (1993), gr-qc/9309025.
- [33] A. D. Linde, Phys. Lett. **B108**, 389 (1982).
- [34] A. Albrecht, P. J. Steinhardt, M. S. Turner, and F. Wilczek, Phys. Rev. Lett. **48**, 1437 (1982).
- [35] A. D. Dolgov and A. D. Linde, Phys. Lett. **B116**, 329 (1982).
- [36] L. F. Abbott, E. Farhi, and M. B. Wise, Phys. Lett. **B117**, 29 (1982).
- [37] J. H. Traschen and R. H. Brandenberger, Phys. Rev. **D42**, 2491 (1990).
- [38] E. W. Kolb and M. S. Turner, Front. Phys. **69**, 1 (1990).
- [39] C. Grojean and G. Servant, Phys. Rev. **D75**, 043507 (2007), hep-ph/0607107.
- [40] URL <http://openmp.org/>.
- [41] M. Frigo and S. G. Johnson, Proceedings of the IEEE **93**, 216 (2005), special issue on "Program Generation, Optimization, and Platform Adaptation".